

Ordering of Poly(*p*-phenylene ethynylene)s in Liquid Crystals

Akihiro Ohira and Timothy M. Swager\*

Department of Chemistry, Massachusetts Institute of Technology, Cambridge, Massachusetts 02139

Received September 1, 2006; Revised Manuscript Received November 4, 2006

**ABSTRACT:** Poly(phenylene ethynylene)s were designed and synthesized that are completely soluble in nematic liquid crystalline solvents at molecular weights (GPC, relative to PS) of more than 100 000. These materials experience a chain extended rod conformation under these conditions with the polymer chains highly aligned with the liquid crystal director and an enhanced conjugation length determined by optical spectroscopy. Structure–property relationships are investigated that reveal the role of steric congestion about the polymer mainchain in determining the order parameter of the polymers. It was also found that the order polymer parameters increased with increasing molecular weights.

## Introduction

The alignment and conformation of conjugated polymer (CP) chains are crucial for their efficient implementation in electrooptical systems such as electroluminescent devices, sensors, and field-effect transistors.<sup>1</sup> High molecular weight CPs, including polythiophenes, polyfluorenes, poly(*p*-phenylene)s (PPPs), poly(phenylene vinylene)s (PPVs), and poly(*p*-phenylene ethynylene)s (PPEs), have finite persistence lengths and exist as flexible coils as opposed to rigid rods in solution.<sup>2</sup> Consequently, the disorder displayed in solution is often transferred to the solid-state structures of CPs, and there is a general lack of long-range molecular order due to conformational disorder in the polymer main chain. The many structural defects in the solid state ultimately result in diminished device performance and limit the ability to study the intrinsic properties of these materials.<sup>3</sup> These characteristics of CP chains strongly depend on the chemical structure<sup>3</sup> and the molecular weight.<sup>4</sup> Several methods have been investigated to obtain the ordered structures of CPs, including the Langmuir–Blodgett (LB) technique,<sup>5,6</sup> mechanical stretching in a transparent polymer matrix,<sup>7</sup> template alignment in uniaxial mesoporous materials,<sup>8</sup> and mesomorphism<sup>9</sup> of the CP main chain or side chains. Nevertheless, the development of versatile methodologies to fabricate solids with well-aligned polymer conformations with optimal electronic delocalization remains a challenge.

We have previously shown that fluorescent dyes, PPEs, and PPVs containing triptycene groups could be aligned along the nematic director in liquid crystals (LCs) due to minimization of “internal free volume”, resulting in significant ordering (high order parameter,  $S$ , and dichroic ratio,  $D$ ).<sup>10,11</sup> More recently, we have succeeded in the demonstration that the organization imparted by a liquid crystal solvent can provide for a substantial enhancement in intrachain energy transfer within iptycene-containing PPEs possessing a low-energy band gap end group. The latter result was attributed to increased conjugation length that accompanies the enhanced alignment of the polymer main chain.<sup>12</sup> In related work, Scholes and co-workers have investigated organizing poly[2-(2'-ethylhexyloxy)-5-methoxy-1,4-phenylenevinylene] (MEH-PPV) with an LC solvent host.<sup>13</sup> However, in these cases which do not contain triptycene groups, much lower degrees of organization are realized.

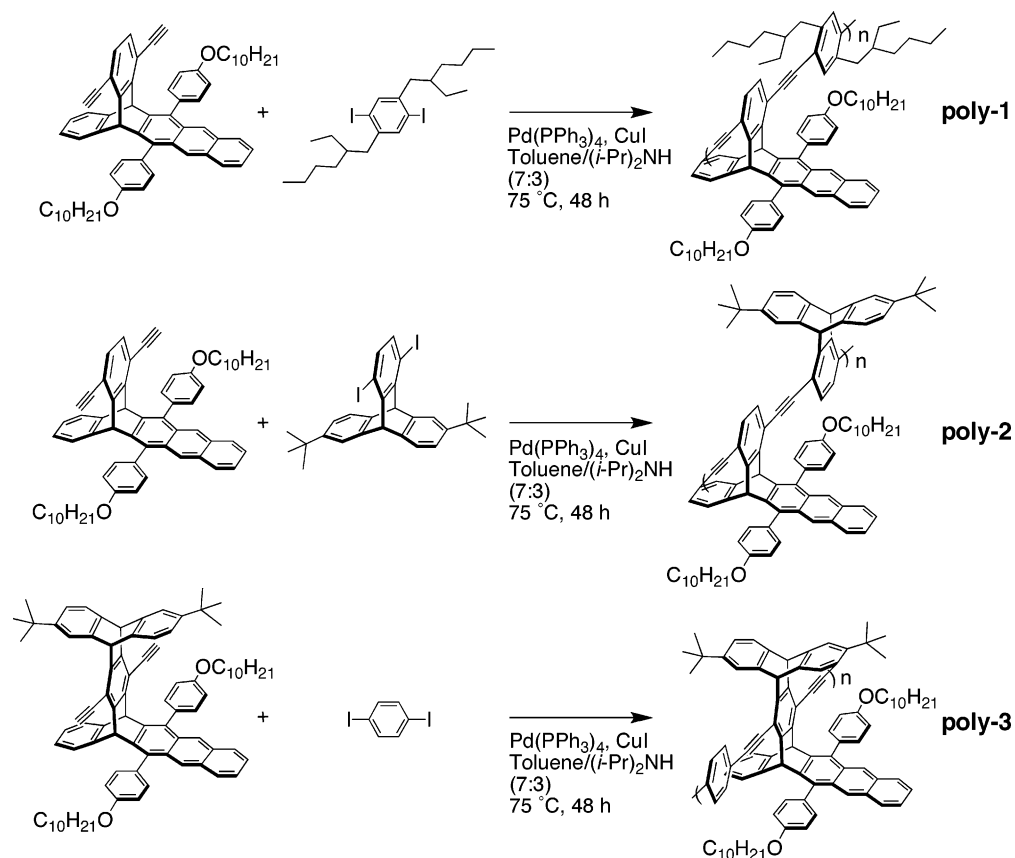
We report herein the synthesis of novel PPEs (**poly-1**, **poly-2**, and **poly-3**, Scheme 1) incorporated with more elaborate

iptycene scaffolds designed to create polymers displaying greater order and enhanced solubility in LCs at high molecular weights. The polymers are produced as soluble stable materials by palladium-catalyzed cross-coupling reactions (Scheme 1). These studies also reveal a molecular weight dependence (degree of polymerization, DP: ca. 10–200) whereby the degree of alignment in the LC system increases linearly with increasing molecular weight.

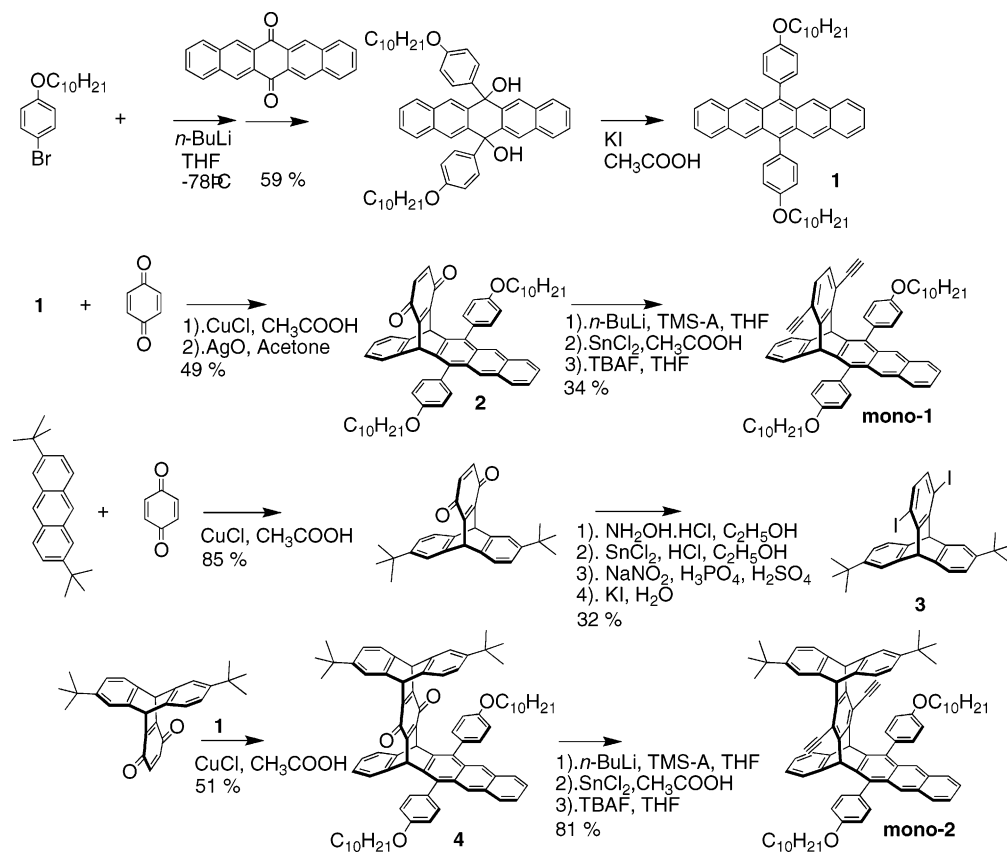
Monomers, **mono-1** and **mono-2** (Scheme 2), were designed to define issues determining the degree of alignment imposed by the iptycene scaffolds. The syntheses, which are shown in Scheme 2, make use of facile Diels–Alder reactions between quinones and a diphenylpentacene. Although the parent unsubstituted pentacene undergoes Diels–Alder additions predominantly at the central ring, the phenyl moieties block this site to give the product shown. The phenyl groups are incorporated by reacting the corresponding aryllithium derivatives with pentacene quinone, followed by reductive deoxygenation to give groups that will become the terphenyl units. These terphenyl units, which are present in both monomers, can be thought of as an incorporated mesogen within the iptycene scaffold that is oriented parallel with the polymer's backbone. These monomers also have an extended planar surface in the form of an anthracene unit that was not present in previous materials. **Mono-1** and **mono-2** were dissolved in an LC host (MLC-6884), which has negative dielectric anisotropy and a nematic phase at room temperature. This LC host transforms to an isotropic liquid at 76.3 °C and 2 wt % solutions homogeneously aligned in rubbed polyimide-coated test cells (10 μm thickness). The UV absorption spectra of **mono-1** and **mono-2** in test cells (Figure 1) reveal a high order parameter  $S_A$  ( $S_{A1}$ : 0.75;  $S_{A2}$ : 0.73) and dichroic ratios  $D_A$  ( $D_{A1}$ : 10.0;  $D_{A2}$ : 9.38). These values are obtained from polarized UV–vis absorbance ratios of the lowest energy 0–0 transition at orientations parallel and perpendicular to the LC director.<sup>16</sup> The intensity at the 0–0 transition was chosen because it is purely associated with the anthracene unit and polarized along the anthracene short axis. These results confirm that **mono-1** and **mono-2** display organizations consistent with our model wherein a plane bisecting the iptycene scaffold is organized perpendicular to the liquid crystal director. In this way the liquid crystal molecules are best aligned to fill the concave surfaces presented by the iptycene and minimize free volume.<sup>10</sup> The order parameters for **mono-1** and **mono-2** are higher than those reported previously for other small molecules by our group.<sup>10</sup> This enhancement is attributed not only to the

\* Corresponding author. E-mail: tswager@mit.edu.

Scheme 1. Chemical Structures of Monomer and Polymers



Scheme 2



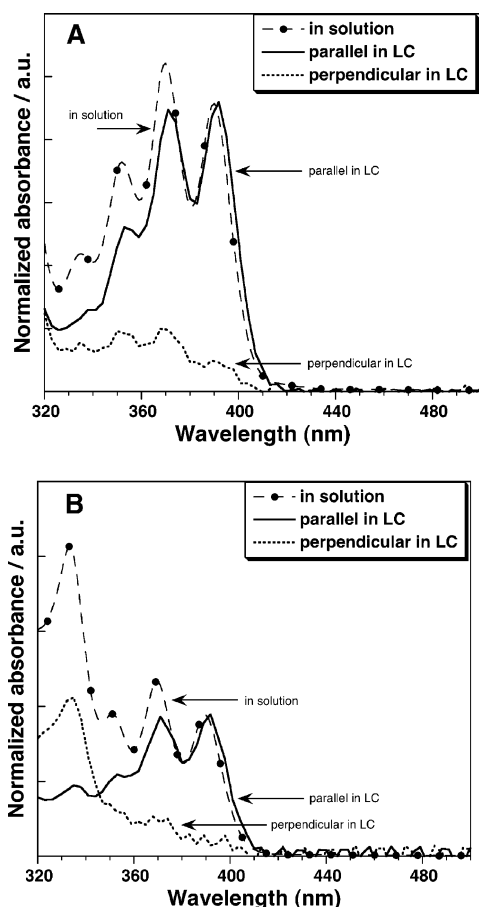


**Figure 1.** UV-vis spectra of **mono-1** (A) and **mono-2** (B) in solution ( $\text{CHCl}_3$ ) and LC. The UV spectra of LC solutions were taken parallel (solid line) and perpendicular (dotted line) to the LC director alignment. The molar extinction coefficient,  $\epsilon$ , was measured in  $\text{CHCl}_3$ , and the  $\epsilon$  values of **mono-1** and **mono-2** at 392 nm were  $1.8 \times 10^4$  and  $1.2 \times 10^4$ , respectively.

effect of internal free volume but also to the terphenyl group. Furthermore, in comparison with these values,  $S$  and  $D$  values of **mono-1** are slightly higher than those of **mono-2**. This is also consistent with our model wherein the less sterically congested iptycene scaffold of **mono-1** is less disruptive to the local LC order than **mono-2**. On the basis of the results obtained from the alignment properties of monomers, we expected that **poly-1**, **poly-2**, and **poly-3** derived from these monomers will display highly extended conformations in liquid crystal solvents.

Figure 2 shows UV-vis absorption and photoluminescence (PL) spectra of **poly-1**, **poly-2**, and **poly-3** observed in solution, spin-cast films, and LC solvent. These polymers readily dissolve in LC solvent (we typically used 1.0 wt % polymer-LC solution system for the experiment). The UV-vis absorption spectra of

**poly-1** and **poly-2** exhibit significant red wavelength shifts in LC solvent ( $\lambda_{\text{max}}$  shifts by 30 and 10 nm, respectively) relative to the spectra observed in dichloromethane solvent. In contrast, **poly-3** exhibits no such shift, and hence it appears that steric crowding in this material restricts the large degree of interaction with the liquid crystal solvent that promotes a planarization of **poly-1** and **poly-2**. Consistent with this decreased interaction with the LC solvent, we find that only relatively low molecular weight chains of **poly-3** completely dissolved in the LC. For **poly-1**, which has the least steric congestion, it is also likely that the conformational preferences of the ethylhexyl (EtH) side chains in the comonomer also promote efficient association with the LC molecule,<sup>11</sup> resulting in the highest  $S$  and  $D$  values ( $S_A$ : 0.86;  $D_A$ : 19.0). The correlation with the degree of alignment with a red-shifting of the absorption  $\lambda_{\text{max}}$  is consistent through the series (Table 1) with **poly-1** displaying the greatest red shift and highest alignment.

The absorption spectra of **poly-1** (Figure 2A) are considerably different in LC solutions relative to isotropic solutions (i.e., dichloromethane). In general, CPs with disordered conformations display spectra that can be described as a collection of chromophores created by a distribution of conjugation lengths. This fact generally leads to broadened absorption spectra. The new sharp absorption band at 422 nm for **poly-1** in LC solvent is not observed in isotropic solutions and thin films, and hence we believe this feature is the result of a uniform and extended conjugation length in the LC solution. Similar features have been observed in organized  $\pi$ -aggregates<sup>6</sup> that have a planarized structure along with interpolymer interactions. Aggregation of this type typically results in greatly reduced emission efficiencies and broadened emission spectra. However, in the case of **poly-1** we observe an emission with similar features in both LC and isotropic solutions, and hence we conclude that there is no intermolecular  $\pi$ -aggregation in LC solutions.

CPs generally display less variation in their emission spectra as a result of facile energy migration to minority segments having extended conjugation and lower bandgaps. Nevertheless, we observe a significant red shift (ca. 6 nm) in the fluorescence spectrum of **poly-1**, in liquid crystal solutions relative to values in dichloromethane solution. The homogeneous chain extended conformation in **poly-1** also leads to a small Stokes shift of 9 nm. Chain alignment determined by polarized emission measurements,  $S_L$  and  $D_L$ , are in agreement with the  $S_A$  and  $D_A$  determined for each polymer (Table 1). This spectral behavior in LC solutions is consistent with the result we have reported previously.<sup>10</sup> It is important to emphasize that we do not see any evidence of strong interpolymer interactions such as  $\pi$ -aggregation. The fluorescence spectra of all of the polymers in LC solutions are similar in shape to that obtained in dichloromethane solution state and are in contrast to the broadened spectra obtained in thin films (Figure 2). Another indication suggestive

**Table 1. Numerical Data for Polymers**

polymer	$M_n^a$ ( $\times 10^4$ )	PDI	abs $\lambda_{\text{max}}$ (nm) <sup>b</sup>	PL $\lambda_{\text{max}}$ (nm) <sup>b</sup>	$\epsilon^c$ ( $\times 10^4$ )	$S_A^d$ (UV)	$D_A^d$ (UV)	$S_L^e$ (PL)	$D_L^e$ (PL)	$\Phi_F$ $\text{CHCl}_3$	$\Phi_F$ solid film
<b>poly-1</b>	2.5	1.2	391 (422)	425 (431)	5.5	0.86	19.0	0.84	17.1	0.67	0.11 (0.02)
<b>poly-2</b>	2.2	1.9	375 (388)	416 (417)	6.1	0.81	13.5	0.81	13.6	0.26	0.11 (0.02)
<b>poly-3</b>	2.2	1.8	411 (411)	421 (421)	6.2	0.80	13.3	0.80	13.3	0.66	0.07 $\pm$ 0.02

<sup>a</sup> Relative to polystyrene standards (GPC). Note that GPC often inflates the values for rigid polymers. <sup>b</sup> Values in  $\text{CHCl}_3$  solution and the corresponding values in MLC-6884 are shown in parentheses. <sup>c</sup> Molar extinction coefficient,  $\epsilon$ , was measured in  $\text{CHCl}_3$ . <sup>d</sup> Obtained by taking an intensity ratio at **poly-1**: 422 nm, **poly-2**: 388 nm, and **poly-3**: 411 nm with the polarizer parallel ( $A_{\parallel}$ ) and perpendicular ( $A_{\perp}$ ) to the LC alignment. The order parameter,  $S_A$ , and dichroic ratio,  $D_A$ , were calculated by the equations  $S_A = (A_{\parallel} - A_{\perp}) / (A_{\parallel} + 2A_{\perp})$  and  $D_A = A_{\parallel} / A_{\perp}$ , respectively. <sup>e</sup> The PL anisotropy,  $S_L$ , and polarized dichroic ratio,  $D_L$ , are defined as  $S_L = (I_{VV} - I_{VH}) / (I_{VV} + 2I_{VH})$  and  $D_L = I_{VV} / I_{VH}$  where the emission intensity,  $I_{VV}$ , is measured with vertically polarized excitation and a vertically polarized emission analyzer and  $I_{VH}$  is measured with vertically polarized excitation and a horizontal emission analyzer. The  $I_{VH}$  was corrected by the  $G$  factor which takes into account the nonideal instrument response. These values here were determined by intensity ratios at 431 nm (**poly-1**), 417 nm (**poly-2**), and 421 nm (**poly-3**) with the analyzer parallel ( $I_{VV}$ ) and perpendicular ( $I_{VH}$ ) to the LC alignment.

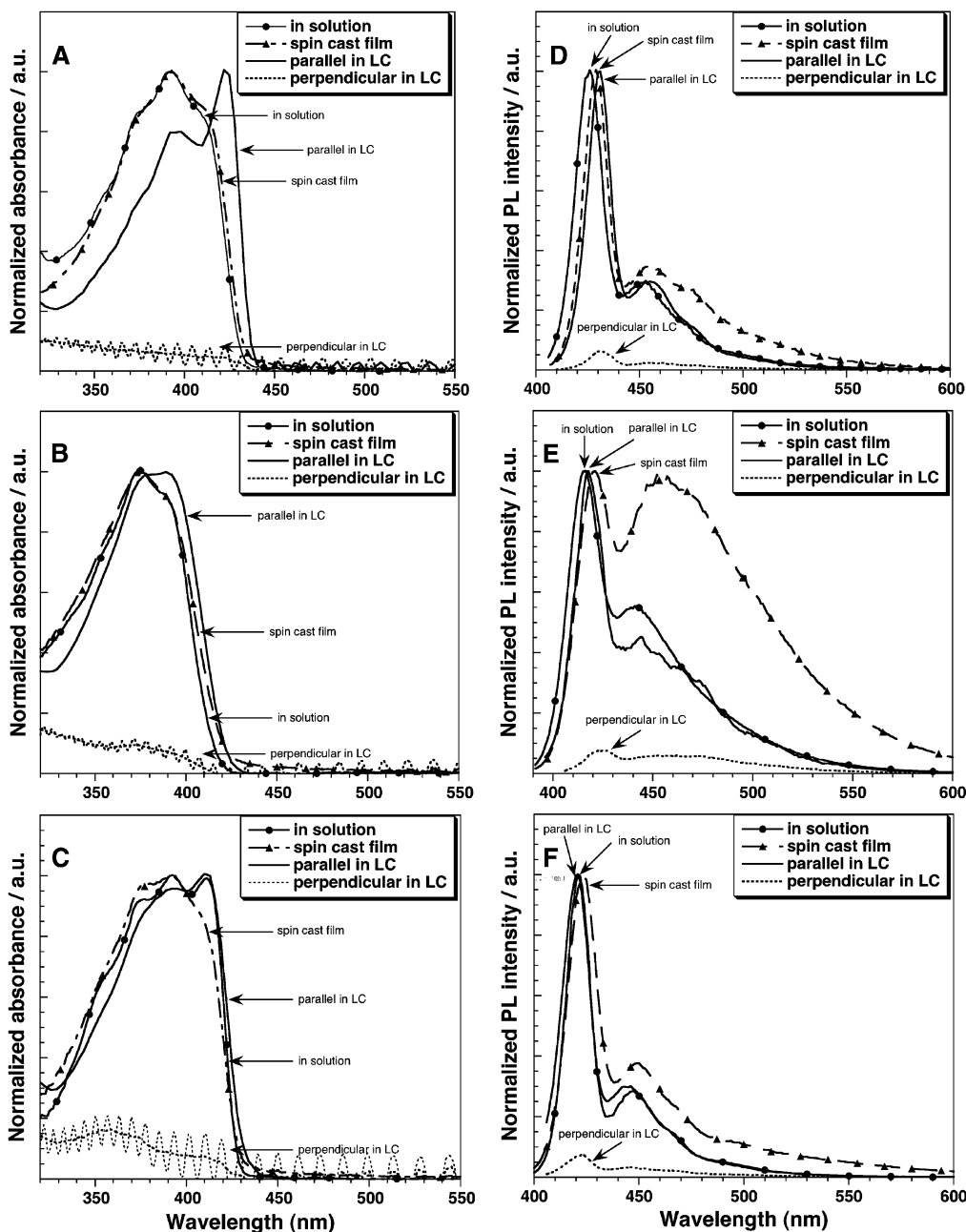


**Figure 2.** UV-vis and photoluminescence in solution, spin-cast film, and LC solutions of **poly-1** (A, D), **poly-2** (B, E), and **poly-3** (C, F). In (A–C), the UV spectra of LC were taken parallel (solid line) and perpendicular (dotted line) to the LC director alignment. In (D–F), photoluminescence spectra of LC were taken with the excitation polarized parallel to the nematic LC director. The solid line shows the emission spectra acquired with the emission channel polarizer parallel to the polarization plane of excitation light, and the dotted line corresponds to the spectrum obtained with the emission channel polarizer perpendicular to one. The spectra corrected to account for instrumental effects ( $G$  factor).

of  $\pi$ -aggregation in thin films is the presence of new absorption features on the red edge of the emission bands, which are assigned to excimer states. The excimer emission is particularly pronounced in the case of **poly-2**.

**Poly-1** displayed superior solubility in liquid crystals, and we found that it was completely soluble over all of the molecular weights investigated. Hence, this material was selected for a study of the role of molecular weight on the degree of alignment. Figure 3 shows plots of  $S$  value as a function of the logarithm of molecular weights of **poly-1**. These results revealed an increase in the alignment ( $S$  and  $D$  values) with increasing molecular weight, thereby indicating that polymer chains are more ordered with increasing molecular weight. Van Der Haegen and co-workers have substantiated that ideal long rods can be ordered better than short rods in an anisotropic phase of a rod-shaped

small molecular solution by theoretical studies on the basis of Onsager theory.<sup>17</sup> However, we note that rigid wormlike polymers generally adopt rodlike architecture in the low molecular weight range, while attaining a random coil conformation in the high molecular weight range wherein their length exceeds their persistence length.<sup>18</sup> We furthermore find that the intensity ratio of absorbance observed at 422 and 391 nm ( $A_{422}/A_{391}$ ) increased with the molecular weight (Figure 3). This also indicates that as molecular weight increases, the conjugation lengths of polymer chains are extended, and this effect suggests that translational diffusion of LC molecules along the polymer backbone is responsible for the greater planarization (Figure 4).

In conclusion, we have demonstrated that a novel PPE incorporating an iptycene scaffold with a terphenyl moiety can be soluble in LCs even at high molecular weights ( $>10^5$  Da)



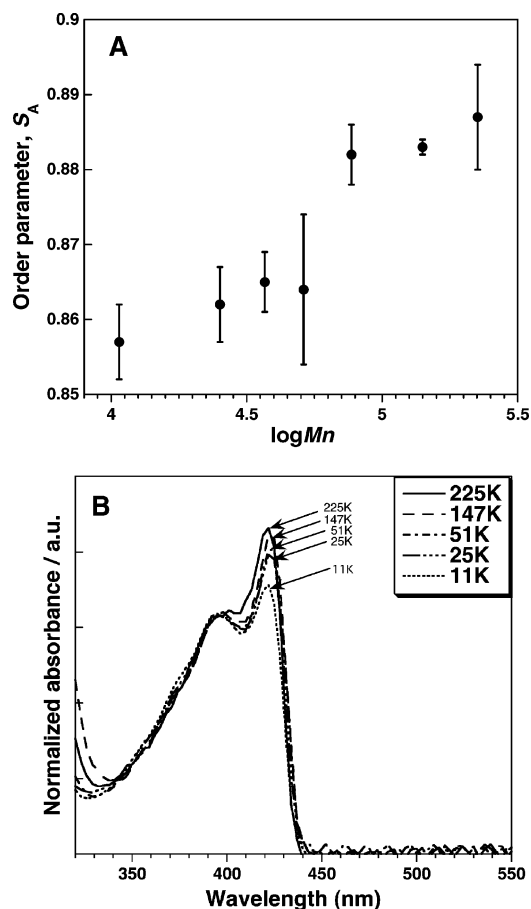


**Figure 3.** (A) Plots of order parameter,  $S_A$ , as a function of molecular weight for **poly-1**. The polydispersity index of all polymers are in the range between 1.2 and 1.8. (B) Polarized UV-vis spectra (normalized at 391 nm) of **poly-1** (taken parallel to the LC director) with various molecular weights in the test cell.

and that the global and local chain conformation can be extended and aligned uniaxially more effectively with increasing molecular weight. The realization of facile and precise alignment control of high molecular weight CPs is crucial to achieve optimal properties. Our future efforts will be focused on using LC alignment to improve the performance of CPs in sensors and organic field effect transistors (OFETs).

### Experimental Procedures

**General.**  $^1\text{H}$  and proton decoupled  $^{13}\text{C}$  NMR spectra were recorded on a Varian MERCURY (300 MHz) instrument, using  $\text{CDCl}_3$  as reference. The chemical shifts were referenced to solvent peaks that had been determined relative to tetramethylsilane (0 ppm). High-resolution mass spectra were obtained with a Bruker Daltonics APEXIV 4.7 T Fourier transform ion cyclotron resonance mass spectrometer (FT-ICR-MS) using an electron impact 70 eV source and a peak matching protocol to determine the mass and error range of the molecular ion. UV-vis absorption spectra were measured with a Cary 50 UV-vis spectrometer equipped with a Cary fiber-optic coupler accessory. Photoluminescence spectra were acquired with a SPEX Fluorolog-2 fluorometer (model FL112, 450 W xenon lamp) equipped with a 1935B polarization kit. The fluorescence anisotropy was determined using a standard procedure.<sup>19</sup> The PL spectra of spin-cast film and LC were recorded in front-face geometry. Solution- and solid-state quantum yields were respectively determined relative to quinine bisulfate in 0.1 N  $\text{H}_2\text{SO}_4$  (solution samples,  $\Phi_F = 0.556$ ) and  $\sim 10$  mM 9,10-diphenylanthracene in PMMA spin-cast film (solid films,  $\Phi_F = 0.837$ ). The molecular weights of polymers were determined by gel permeation chromatography (GPC) relative to polystyrene standards (Poly-

Sciences) with THF as the eluent and a Hewlett-Packard series 1100 HPLC equipped with a Plgel 5 mm Mixed-C ( $300 \times 7.5$  mm) column. Reagents were purified and dried by standard techniques, and all air- and water-sensitive synthetic manipulations were performed under an argon atmosphere using standard Schlenk techniques. The host liquid crystal MLC-6884 was purchased from Merck Chemicals Ltd. Monomer (2.0 wt %) and polymer (1.0 wt %) LC solutions were prepared using the following procedure: A 2.0 mg sample of monomer was taken and added to 98 mg of MLC-6884 in a small vial with 2.0 mL of chloroform. The chloroform was evaporated at reduced pressure, and the solution was heated into the isotropic phase with a heat gun for 15 s. Cooling to room temperature resulted in generation of a homogeneous LC solution. Polymer-LC solutions were prepared in the same way except with 1 mg of polymer being dissolved in 99 mg of LC. Solutions were heated to 85 °C with a Linkham 350 hot stage (the clearing point of MLC-6884 is 76.3 °C) and infused by capillary action into KSRO-10 test cells (cell gap 10  $\mu\text{m}$ , with parallel rubbed polyimide coating, manufactured by E.H.C. Co. Ltd, Japan). The cell was slowly cooled to 75 °C, equilibrated at this temperature for 30 min, and then slowly cooled to room temperature. Different molecular weight polymer samples were prepared by fractional precipitation. Polymer (200 mg) was dissolved in 30 mL of toluene, and then 2 mL of ethanol and 1 mL of methanol were added slowly. The methanol induced precipitates and solids were separated by centrifugation and decanting. By this procedure, we successfully obtained low-polydispersity polymers with molecular weights ranging from 10K to over 200K.

**Synthesis of 6,13-Dihydroxy-6,13-bis(decyloxyphenyl)-6,13-dihydropentacene.** A solution of *n*-BuLi (40 mL of 1.6 M solution in hexanes, 63.0 mmol) was added dropwise to a  $-78$  °C stirred solution of 20 g (63.0 mmol) of 4-bromodecoxybenzene and 7.32 g (9.45 mL, 63.0 mmol) of *N,N,N',N'*-tetramethylethylenediamine (TMEDA) in 60 mL of THF. The solution was stirred for 2.0 h at  $-78$  °C, followed by addition of a solution of 6.5 g (21 mmol) of 6,13-pentacenequinone in 60 mL of THF. This reaction mixture was stirred for 1.0 h at  $-78$  °C and further stirred at room temperature for 12 h. At this time 50 mL of 10% hydrochloric acid solution was added and followed by an aqueous work up with dichloromethane. The organic fraction was successively washed with water and saturated  $\text{NH}_4\text{Cl}$  solution and dried over  $\text{MgSO}_4$ . After concentration in vacuo, the crude product was a yellow solid which was purified by chromatography on silica gel with a gradient eluent of 100% hexanes to 100% dichloromethane and then recrystallized from hexane to give 9.66 g (59%) of light yellow solid.  $^1\text{H}$  NMR (300 MHz,  $\text{CDCl}_3$ ): 8.35 (s, 4H), 7.84 (dd, 4H), 7.51 (dd, 4H), 6.27 (d, 4H), 5.91 (d, 4H), 3.66 (s, 2H), 3.54 (t, 4H), 1.62 (m, 4H), 1.42–1.27 (m, 28H), 0.87 (t, 6H).  $^{13}\text{C}$  NMR (75 MHz,  $\text{CDCl}_3$ ): 14.1, 22.6, 26.0, 29.2, 29.3, 29.5, 29.6, 31.9, 67.8, 75.7, 112.9, 124.6, 126.0, 128.1, 128.8, 132.5, 134.0, 139.4, 157.2. HRMS calcd for  $\text{C}_{54}\text{H}_{64}\text{O}_4\text{Na}$  ( $M + \text{Na}$ ) $^+$ , 799.4697; found 799.4692.

**Synthesis of 6,13-Bis(decyloxyphenyl)pentacene (1).** A mixture of 9.5 (12.2 mmol) g of 6,13-dihydroxy-6,13-bis(decyloxyphenyl)-6,13-dihydropentacene and 8.1 g (48.8 mmol) of potassium iodide in 200 mL of glacial acetic acid was refluxed for 2.0 h in the dark (note, we observed product degradation with laboratory light) and then allowed to cool with the addition of 250 mL of water. The reddish-purple solid was generated and filtered then washed with methanol and water several times in the dark. Because of its sensitivity, this compound was carried immediately to the next step without further purification.

**Synthesis of 2.** In 200 mL of glacial acetic acid, crude of **1** (9.0 g, 12.0 mmol), *p*-benzoquinone (1.69 g, 15.7 mmol), and CuCl (1.12 g, 12.0 mmol) were combined, and the solution was heated to reflux for 1.5 h in the dark. The reaction was cooled and quenched by pouring into water. The precipitate was filtered, washed with hot water, dissolved in dichloromethane, and dried over  $\text{MgSO}_4$ . After concentration in vacuo, the crude product was dissolved in acetone, and 5.9 g of AgO (48 mmol) was added into solution followed by stirring for 12 h in the dark. The solution was then dissolved in

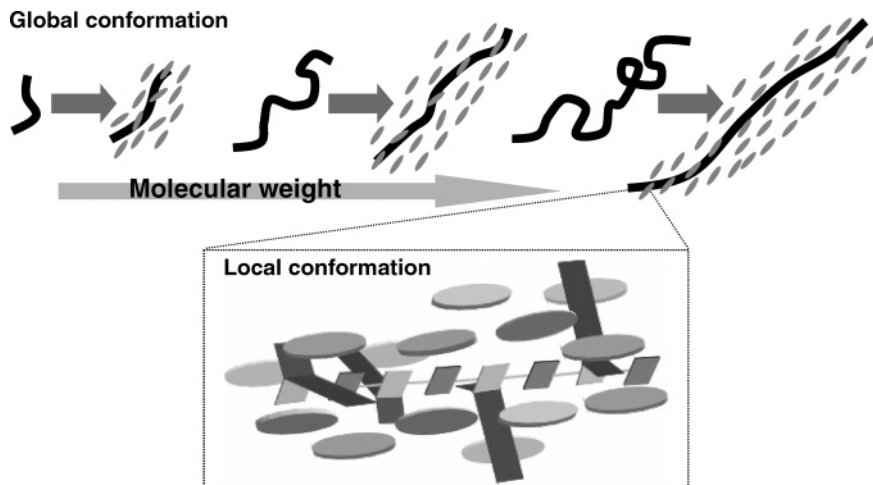


**Figure 4.** Schematic representation of global and local conformation of **poly-1** in LC solution.

dichloromethane, filtered through a plug of celite, and dried over  $\text{MgSO}_4$ . After concentration in vacuo, a dark brown solid was purified by chromatography on silica gel (eluent dichloromethane: hexane 30:70). Recrystallization from methanol gave 5.0 g (49%) of **2** as a red solid.  $^1\text{H}$  NMR (300 MHz,  $\text{CDCl}_3$ ): 8.07 (s, 2H), 7.76 (dd, 2H), 7.37 (dd, 2H), 7.31 (m, 4H), 7.20 (dd, 4H), 7.07 (dd, 2H), 6.93 (dd, 2H), 6.64 (s, 2H), 5.85 (s, 2H), 4.21 (m, 4H), 1.98 (m, 4H), 1.66–1.31 (m, 28H), 0.95 (t, 6H).  $^{13}\text{C}$  NMR (75 MHz,  $\text{CDCl}_3$ ): 183.8, 158.9, 150.8, 142.8, 137.4, 135.6, 135.5, 134.5, 131.8, 131.4, 130.2, 129.4, 128.1, 126.0, 125.6, 125.3, 124.5, 114.8, 114.5, 68.1, 44.8, 31.9, 29.7, 29.6, 29.5 (2 peaks), 29.4, 26.2, 22.7, 14.2. HRMS calcd for  $\text{C}_{60}\text{H}_{64}\text{O}_4\text{Na}$  ( $\text{M} + \text{Na}$ ) $^+$ , 871.4697; found 871.4664.

**Synthesis of Mono-1.** A solution of *n*-BuLi (4.4 mL of 1.6 M solution in hexanes, 7.02 mmol) was added dropwise to a  $-78^\circ\text{C}$  stirred solution of 0.69 g (0.99 mL, 7.02 mmol) of (trimethylsilyl)acetylene in 10 mL of THF. The resulting solution was stirred for 1.5 h at  $-78^\circ\text{C}$ , and 1.5 g (1.75 mmol) of **2** in 5 mL of THF was then added. The reaction mixture was stirred for 30 min at  $-78^\circ\text{C}$  and further stirred at room temperature for 24 h. Then 2.38 g (10.5 mmol) of stannous chloride in 10 mL of 10% hydrochloric acid was added dropwise to the solution. The reaction mixture was stirred for 24 h, diluted with water, and extracted with dichloromethane. The organic fraction was washed successively with saturated  $\text{NH}_4\text{Cl}$  solution and water and dried over  $\text{MgSO}_4$ . Concentration in vacuo gave 0.91 g of a crude disilyl-protected **mono-1** as a yellow solid material. To remove the TMS protecting groups from the acetylene, this intermediate was dissolved in 50 mL of THF, and 1.2 g of TBAF (75% solution in water) was added. The resulting solution was stirred at room temperature for 1 h, poured into water, and extracted with dichloromethane. The organic fraction was successively washed with saturated  $\text{NH}_4\text{Cl}$  solution and water and dried over  $\text{MgSO}_4$ . After concentration in vacuo, the crude dark yellow solid was purified by chromatography on silica gel (eluent dichloromethane: hexane 30:70) to give 0.525 g (34%) of **mono-1** as a yellow solid.  $^1\text{H}$  NMR (300 MHz,  $\text{CDCl}_3$ ): 8.17 (s, 2H), 7.78 (dd, 2H), 7.51 (dd, 2H), 7.40 (dd, 2H), 7.33 (m, 4H), 7.22 (d, 4H), 7.15 (s, 2H), 7.07 (dd, 2H), 5.98 (s, 2H), 4.16 (m, 4H), 3.23 (s, 2H), 1.93 (m, 4H), 1.67–1.30 (m, 28H), 0.93 (t, 6H).  $^{13}\text{C}$  NMR (75 MHz,  $\text{CDCl}_3$ ): 158.6, 147.1, 143.8, 137.5, 133.5, 132.9, 131.7, 131.2, 130.4, 130.2, 128.8, 128.1, 125.9, 125.5, 125.0, 124.1, 118.1, 114.5, 114.2, 82.1, 80.8, 68.2, 48.9, 31.9, 29.7, 29.6, 29.5 (2 peaks), 29.4, 26.2, 22.7, 14.2. HRMS calcd for  $\text{C}_{64}\text{H}_{66}\text{O}_2\text{Na}$  ( $\text{M} + \text{Na}$ ) $^+$ , 889.4955; found 889.4975.

**Synthesis of 1,4-Diiodo-6,11-di(*tert*-butyl)tritycene (3).** The dioxime of 6,11-di(*tert*-butyl)tritycenequinone was prepared by 2.0 h of reflux of a solution of 1.0 g (2.54 mmol) of 6,11-di(*tert*-butyl)tritycenequinone<sup>12</sup> and 2.82 g (40.6 mmol) of hydroxylamine hydrochloride in 100 mL of ethanol. The dioxime was isolated by pouring into water and washed with hot water. The crude orange

solid was used for the next step. Reduction of the dioxime to the diamine was accomplished by the following procedure; 1.0 g (2.35 mmol) of the dioxime was dissolved in 15 mL of ethanol, and then 15 mL of concentrated hydrochloric acid was added. After the mixture changed to a homogeneous solution, 3.2 g (14.1 mmol) of stannous chloride was added with stirring. The mixture was refluxed for an additional 45 min and then poured into water. The solid was precipitated and washed with hot water, dissolved in ethyl acetate, and dried over  $\text{MgSO}_4$ . After concentration in vacuo, a hydrochloride salt of the diamine was isolated and used without purification in the next step. A suspension of the crude hydrochloride salt (0.91 g, 1.98 mmol) in 30 mL of phosphoric acid cooled to  $0^\circ\text{C}$  was added to a similarly cooled mixture of 20 mL of acetic acid and 14 mL of water. A solution of sodium nitrite (0.82 g, 11.9 mmol) in 25 mL of concentrated sulfuric acid was slowly added to this solution, with care being taken to maintain the temperature below  $0^\circ\text{C}$ . The resulting red solution was stirred at  $0^\circ\text{C}$  for 1.5 h and then poured into an aqueous solution of potassium iodide (5.0 g in 50 mL). This mixture was stirred at room temperature for 12 h. The solid product was collected via filtration, washed with water and saturated  $\text{Na}_2\text{S}_2\text{O}_3$  solution, and then purified by column chromatography on silica gel (eluent hexane 100%). The product, **3**, was then recrystallized from ethanol to yield 0.38 g of a white solid (32% yield).  $^1\text{H}$  NMR (300 MHz,  $\text{CDCl}_3$ ): 7.49 (d, 2H), 7.39 (d, 2H), 7.11 (s, 2H), 7.06 (dd, 2H), 5.72 (s, 2H), 1.29 (s, 18H).  $^{13}\text{C}$  NMR (75 MHz,  $\text{CDCl}_3$ ): 31.5, 34.6, 58.7, 94.1, 121.3, 122.3, 123.4, 136.2, 141.4, 144.2, 148.8, 150.3. HRMS calcd for  $\text{C}_{28}\text{H}_{28}\text{I}_2$  ( $\text{M}^+$ ), 618.0275; found 618.0299.

**Synthesis of 4.** In 140 mL of glacial acetic acid were added **1** (1.70 g, 2.28 mmol), 6,11-di(*tert*-butyl)tritycenequinone (1.17 g, 2.97 mmol), and  $\text{CuCl}$  (0.22 g, 2.22 mmol). The solution was then heated to reflux for 2 h in the dark. The reaction was cooled and quenched by pouring into water. The precipitate was filtered, washed with water, dissolved in dichloromethane, and dried over  $\text{MgSO}_4$ . After concentration in vacuo, a dark brown solid was purified by chromatography on silica gel (eluent dichloromethane: hexane 25:75) to yield 1.32 g (51%) of **4** as a dark red solid.  $^1\text{H}$  NMR (300 MHz,  $\text{CDCl}_3$ ): 8.06 (d, 2H), 7.79 (dd, 2H), 7.41 (d, 1H), 7.31–7.16 (m, 15H), 6.98 (m, 3H), 6.94 (d, 1H), 5.75 (d, 2H), 5.69 (s, 2H), 4.19 (m, 4H), 1.95 (m, 4H), 1.69–1.33 (m, 28H), 1.20 (s, 18H), 0.93 (t, 6H).  $^{13}\text{C}$  NMR (75 MHz,  $\text{CDCl}_3$ ): 180.2 (2 peaks), 158.9, 151.4 (2 peaks), 149.7, 148.6 (2 peaks), 143.8, 143.7, 143.1, 143.0, 140.9, 140.8, 135.7, 134.3, 131.9, 131.8, 131.5, 131.4, 131.3, 130.2 (2 peaks), 129.6 (2 peaks), 128.1, 125.9, 125.5, 125.1, 124.3, 121.9, 114.8, 114.4, 68.1, 47.4, 44.8, 34.6, 34.5, 32.0, 31.4 (2 peaks), 29.7 (2 peaks), 29.6, 29.5, 29.4, 26.3, 22.7, 14.2. HRMS calcd for  $\text{C}_{82}\text{H}_{88}\text{O}_4\text{Na}$  ( $\text{M} + \text{Na}$ ) $^+$ , 1159.6575; found 1159.6592.

**Synthesis of Mono-2.** A solution of *n*-BuLi (1.53 mL of 1.6 M solution in hexanes, 2.45 mmol) was added dropwise to a stirred at  $-78^\circ\text{C}$  solution of 0.241 g (0.35 mL, 2.45 mmol) of (trimeth-

ylsilyl)acetylene in 5 mL of THF. The resulting solution was stirred for 1.5 h at  $-78\text{ }^{\circ}\text{C}$ , and then 0.70 g (0.61 mmol) of **4** in 3 mL of THF was added into the solution. The reaction mixture was stirred for 30 min at  $-78\text{ }^{\circ}\text{C}$  and further stirred at room temperature for 24 h. Stannous chloride in 10 mL of 10% hydrochloric acid was then added dropwise to the solution. The reaction mixture was stirred for 24 h, then diluted with water, and extracted with dichloromethane, and the organic fraction was washed successively with saturated  $\text{NH}_4\text{Cl}$  solution and water and dried over  $\text{MgSO}_4$ . Concentration in vacuo gave 0.75 g of crude disilyl-protected **4** as a dark yellowish solid. Deprotection was accomplished by dissolving the crude product in 50 mL of THF and adding 0.60 g of TBAF (75% solution in water). The resulting solution was stirred at room temperature for 1 h, washed with water, and then extracted with dichloromethane. The organic fraction was successively washed with saturated  $\text{NH}_4\text{Cl}$  solution and water and dried over  $\text{MgSO}_4$ . After concentration in vacuo, the crude product as a dark yellow solid was purified by chromatography on silica gel (eluent dichloromethane:hexane 25:75) to yield 0.54 g (81%) of **4** as a yellow solid.  $^1\text{H}$  NMR (300 MHz,  $\text{CDCl}_3$ ): 8.05 (d, 2H), 7.79 (dd, 2H), 7.56–7.17 (m, 16H), 6.98 (m, 3H), 6.93 (d, 1H), 5.91 (s, 2H), 5.79 (s, 2H), 4.23 (m, 4H), 3.51 (s, 2H), 2.01 (m, 4H), 1.69–1.33 (m, 28H), 1.28 (s, 18H), 1.01 (t, 6H).  $^{13}\text{C}$  NMR (75 MHz,  $\text{CDCl}_3$ ): 158.6, 148.3, 148.2, 145.4 (2 peaks), 144.8, 144.7, 144.3, 144.2, 143.5, 142.0, 141.9, 137.7, 133.2 (2 peaks), 132.9, 131.7, 131.1, 130.4, 130.3, 128.1, 125.7, 125.4, 124.9, 123.9, 123.3, 123.1, 121.9, 121.3, 114.5, 114.4, 114.2, 114.1, 84.6, 78.9, 68.2, 51.9, 49.1, 34.5 (2 peaks), 32.0, 31.5 (2 peaks), 29.7 (2 peaks), 29.6, 29.5, 29.4, 26.2, 22.7, 14.2. HRMS calcd for  $\text{C}_{86}\text{H}_{91}\text{O}_2$  (M + H), 1155.7014; found 1155.7008.

**Polymer Syntheses.** A general procedure is described by the synthesis of **Poly-1. Mono-1** (150 mg, 0.115 mmol), 1,4-bis(2-ethylhexyl)-2,5-diiodobenzene (93 mg, 0.112 mmol), and  $\text{CuI}$  (0.96 mg) were placed in a Schlenk tube with a stir bar. The flask was evacuated and backfilled with argon three times before the addition of degassed toluene/diisopropylamine (7:3, v/v, 4.0 mL) under an argon atmosphere. The tube was then sealed and subjected to three freeze–vacuum cycles, each time backfilling with argon. At this time 5.9 mg (0.003 mmol) of  $\text{Pd}(\text{PPh}_3)_4$  was added to the tube, and mixture solution was stirred and heated at  $75\text{ }^{\circ}\text{C}$  for 2 days. To work up the reaction, water was added and the polymer was extracted with chloroform. The organic layer was washed successively with saturated  $\text{NH}_4\text{Cl}$  solution and water and dried over  $\text{MgSO}_4$ . The solvent was removed in vacuo. The residue was dissolved in a minimum amount of toluene and filtered by 0.45  $\mu\text{m}$  pore-sized membrane filter to remove small amount of residue solids that are potentially physically or chemically cross-linked polymer. The filtrate was reprecipitated in acetone. The precipitate was washed with acetone five times to give **poly-1** as a yellow solid (52%).  $^1\text{H}$  NMR (300 MHz,  $\text{CDCl}_3$ ): 8.03 (br, s, 2H), 7.77 (br, s, 2H), 7.34 (br, 14H), 6.77–6.62 (br, 4H), 6.25 (br, s, 2H), 3.83–2.66 (br, m, 8H), 1.85 (br, 6H), 1.46–0.77 (br, m, 62H).

Polymers **poly-2** and **poly-3** were synthesized using the similar procedure for **poly-1**. Polymer **poly-2** (55%):  $^1\text{H}$  NMR (300 MHz,  $\text{CDCl}_3$ ): 8.08 (br, 2H), 7.80–7.08 (br, m, 26H), 6.23 (br, 2H), 6.02 (br, 2H), 3.93 (br, 4H), 2.00 (br, 4H), 1.60–0.83 (br, m, 52H). Polymer **poly-3** (60%):  $^1\text{H}$  NMR (300 MHz,  $\text{CDCl}_3$ ): 8.09 (br, s, 2H), 7.81–7.09 (br, m, 26H), 6.24 (br, 2H), 6.03 (br, 2H), 3.94 (br, 4H), 2.01 (br, 4H), 1.64–0.83 (br, m, 52H).

**Acknowledgment.** Akihiro Ohira thanks Mr. Takeshi Igarashi, Mr. Andrew Satrijo, and Drs. Craig A. Breen and Sandra Rifai for fruitful discussions. This research was supported by the National Science Foundation under Grant DMR-0314421

and the Japan Society for the Promotion of Science (Fellowship No. 01682).

**Supporting Information Available:** NMR spectra of the monomers. This material is available free of charge via the Internet at <http://pubs.acs.org>.

## References and Notes

- (1) Conwell, E. M. In *Handbook of Organic Conductive Molecules and Polymers*; Nalwa, H. S., Ed.; John Wiley: New York, 1997; Vol. 4, pp 1–45.
- (2) (a) Cotts, P. M.; Swager, T. M.; Zhou, Q. *Macromolecules* **1996**, *29*, 7323–7328. (b) Fytas, G.; Nothofer, H. G.; Scherf, U.; Vlassopoulos, D.; Meier, G. *Macromolecules* **2002**, *35*, 481–488.
- (3) Bao, Z. N.; Rogers, J. A.; Katz, H. E. *J. Mater. Chem.* **1999**, *9*, 1895–1904.
- (4) (a) Donley, C. L.; Zaumseil, J.; Andreasen, J. W.; Nielsen, M. M.; Sirringhaus, H.; Friend, R. H.; Kim, J.-S. *J. Am. Chem. Soc.* **2005**, *127*, 12890–12899. (b) Kline, R. J.; McGehee, M. D.; Kadnikova, E. N.; Liu, J. S.; Fréchet, J. M. J.; Toney, M. F. *Macromolecules* **2005**, *38*, 3312–3319.
- (5) Reitzel, N.; Greve, D. R.; Kjaer, K.; Howes, P. B.; Jayaraman, M.; Savoy, S.; McCullough, R. D.; McDevitt, J. T.; Bjørnholm, T. *J. Am. Chem. Soc.* **2000**, *122*, 5788–5800.
- (6) (a) Kim, J.; Swager, T. M. *Nature (London)* **2001**, *411*, 1030–1034. (b) Kim, J.; Levitsky, I. A.; McQuade, D. T.; Swager, T. M. *J. Am. Chem. Soc.* **2002**, *124*, 7710–7718.
- (7) Weder, C.; Sarwa, C.; Montali, A.; Bastiaansen, C.; Smith, P. *Science* **1998**, *279*, 835–837.
- (8) (a) Nguyen, T.-Q.; Wu, J. J.; Doan, V.; Schwartz, B. J.; Tolbert, S. H. *Science* **2000**, *288*, 652–656. (b) Hulvat, J. F.; Stupp, S. I. *Adv. Mater.* **2004**, *16*, 589–592. (c) Hulvat, J. F.; Stupp, S. I. *Angew. Chem., Int. Ed.* **2003**, *42*, 778–781.
- (9) (a) Ozaki, M.; Fujisawa, T.; Fujii, A.; Tong, L.; Yoshino, K.; Kijima, M.; Kinoshita, I.; Shirakawa, H. *Adv. Mater.* **2000**, *12*, 587–589. (b) Kuroda, H.; Goto, H.; Akagi, K.; Kawaguchi, A. *Macromolecules* **2002**, *35*, 1307–1313. (c) Banach, M. J.; Friend, R. H.; Sirringhaus, H. *Macromolecules* **2003**, *36*, 2838–2844.
- (10) (a) Long, T. M.; Swager, T. M. *Adv. Mater.* **2001**, *13*, 601–604. (b) Long, T. M.; Swager, T. M. *J. Am. Chem. Soc.* **2002**, *124*, 3826–3827.
- (11) Zhu, Z.; Swager, T. M. *J. Am. Chem. Soc.* **2002**, *124*, 9670–9671.
- (12) Nesterov, E. E.; Zhu, Z.; Swager, T. M. *J. Am. Chem. Soc.* **2005**, *127*, 10083–10088.
- (13) (a) Fritz, K. P.; Scholes, G. D. *J. Phys. Chem. B* **2003**, *107*, 10141–10147. (b) Lammi, R. K.; Fritz, K. P.; Scholes, G. D.; Barbara, P. F. *J. Phys. Chem. B* **2004**, *108*, 4593–4596.
- (14) (a) Knaapila, M.; Kisko, K.; Lyons, B. P.; Stepanyan, R.; Foreman, J. P.; Seeck, O. H.; Vainio, U.; Pålsson, L.-O.; Serimaa, R.; Torkkeli, M.; Monkman, A. P. *J. Phys. Chem. B* **2004**, *108*, 10711–10720. (b) Knaapila, M.; Stepanyan, R.; Lyons, B. P.; Torkkeli, M.; Hase, T. P. A.; Serimaa, R.; Güntner, R.; Seeck, O. H.; Scherf, U.; Monkman, A. P. *Macromolecules* **2005**, *38*, 2744–2753.
- (15) (a) Zhou, Q.; Swager, T. M. *J. Am. Chem. Soc.* **1995**, *117*, 7017–7018. (b) Swager, T. M. *Acc. Chem. Res.* **1998**, *31*, 201–207. (c) McQuade, D. T.; Pullen, A. E.; Swager, T. M. *Chem. Rev.* **2000**, *100*, 2537–2574.
- (16) Polarized UV–vis spectra, parallel,  $A_{||}$ , and perpendicular,  $A_{\perp}$ , to the LC alignment, were recorded and their observed order parameters calculated according to following equation:  $S = (A_{||} - A_{\perp}) / (A_{||} + 2A_{\perp})$ . The dichroic ratio  $D$  is defined as the ratio between the absorption spectrum recorded using light polarized parallel to and perpendicular to the molecular orientation:  $D = A_{||} / A_{\perp}$ . The order parameter,  $S$ , and dichroic ratio,  $D$ , are estimated by taking the intensity ratio at the transition moment of lowest energy vibronically coupled absorption (**mono-1**: 392 nm; **mono-2**: 392 nm) with the polarizer oriented parallel and perpendicular to the LC alignment.
- (17) Lekkerkerker, H. N. W.; Coulon, P.; Van Der Haegen, R.; Deblieck, R. *J. Chem. Phys.* **1984**, *80*, 3427–3433.
- (18) Khokolov, A. R. In *Liquid Crystallinity in Polymers: Principles and Fundamental Properties*; Ciferri, A., Ed.; VHC: New York, 1991; Chapter 3.
- (19) Breen, C. A.; Deng, T.; Breiner, T.; Thomas, E. L.; Swager, T. M. *J. Am. Chem. Soc.* **2003**, *125*, 9942–9943.

MA0620262